

# ULTRASONIC GUIDED WAVES FOR INSPECTION OF BONDED PANELS

D C Price, B J Martin and D A Scott  
CSIRO Telecommunications and Industrial Physics  
Lindfield, NSW

**ABSTRACT:** This paper describes the propagation of "leaky" guided ultrasonic waves in layered planar structures, typical of adhesively bonded metal panels, when they are immersed in water. An outline of the physics of these waves is given, and the way in which they can be used to detect bond defects is indicated.

## 1. INTRODUCTION

Ultrasound is an important tool for characterising engineering materials, both for detecting discrete defects (cracks, voids, disbands, inclusions, etc.) and for assessing material properties (e.g. elastic modulus, microstructure). It is widely used in industry, most commonly in the so-called pulse-echo configuration in which a single piezoelectric transducer, coupled to the surface of the material of interest, is used to excite a longitudinally-polarised pulse of ultrasound, and to detect signals subsequently back-scattered from structures within the material.

There are, however, a significant number of applications in which the material to be evaluated forms a structure in which at least one dimension is much smaller than another and which can, under appropriate circumstances, behave as a waveguide. Planar structures in which the thickness is much smaller than the lateral dimensions constitute an important class of such structures. Ultrasonic inspection of multi-layered planar structures is frequently required in, for example, the aerospace industry: examples are fuselage, wing and control surface skins, multi-layered carbon fibre composite laminates, adhesively bonded lap joints. In cases such as these it is often advantageous to make use of the guided modes that propagate in the structure, both from the point of view of the ability to excite specific dynamic stress distributions in the structure and/or to allow more rapid inspection of relatively large areas. Some examples of the use of ultrasonic Lamb waves, for which the particle motion in the wave is in a plane normal to the plate surface, have been described by Bowles and Scala [1]. A comprehensive review of guided waves in plates, and their use for materials evaluation, has been recently published by Chimenti [2].

This paper is concerned with leaky guided waves in planar structures. Whereas "true" guided waves are free vibrational modes of an elastic structure in vacuum, leaky waves are analogous modes that can be generated when the plate is immersed in a fluid, which may typically be air or water. These waves are excited by an incident wave from the fluid, and they decay by re-radiating (or "leaking") energy into the fluid on both sides of the plate. Mathematically, the difference is that the true guided waves are the solution of the vibrational

eigenvalue problem for the plate, while the leaky waves correspond to the solution of the related scattering problem. If the fluid loading is light (i.e. the acoustic impedance of the fluid is much less than that of the plate) the leaky guided modes are very similar in structure and frequency to the true guided modes. This is normally the case for metals immersed in air or water, but it is not necessarily so for polymer-based materials in water.

The work described in this paper has been carried out over a number of years, as part of a collaboration between CSIRO and the Boeing Commercial Airplane Group. Most of it has not been published in the open literature. The physics of leaky guided waves is not new, though some aspects have not been previously reported. It is believed that the methods utilized here for presentation of the results provide useful insights into the way in which these waves propagate, and interact with an external wave field, and suggest novel methods for the development of defect detection strategies.

In the subsequent sections of this paper a brief introduction will be given to the leaky guided waves in an aluminium plate immersed in water, since water is often used as a coupling medium for ultrasound, particularly in laboratory studies. This will then be extended to consideration of an aluminium/epoxy/aluminium bonded structure, with a description of the way in which these waves are used to detect defective conditions in the bond-line.

The results described in this paper are derived from numerical calculations, but it is important to point out that all of them have been verified by experimental measurement. Some examples of experimental results are included. The overall aim of the program is to develop practical measurement techniques and procedures for characterisation of materials and structures, and for defect detection, and the parallel theoretical and experimental approach adopted is considered to be essential.

## 2. LEAKY GUIDED WAVES IN AN IMMERSSED ALUMINIUM PLATE

Consider a flat sheet of aluminium immersed in water, as shown in Figure 1. An ultrasonic wave of frequency  $f$  is incident on the plate at angle  $\theta$ , in the  $(x, z)$  plane of a

Cartesian coordinate system. It is assumed that the material properties are homogeneous and isotropic, so the elastic properties of the plate are isotropic in the  $(x, y)$  plane; the  $x$ -direction is determined by the incident plane.

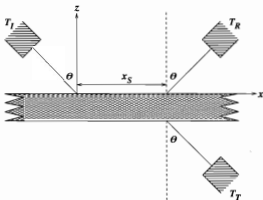


Figure 1. Schematic diagram of the experimental arrangement for generating and detecting leaky guided waves in a planar material. An incident ultrasonic wave is emitted by the transducer  $T_I$ , and waves reflected from and transmitted through the plate are detected by transducers  $T_R$  and  $T_T$ , respectively. The distance  $x_s$  is known as the transducer separation: if  $x_s = 0$ , direct reflection and transmission are measured.

The scattered wave field may be calculated by the following general procedure.

- Initially consider that the incident wave is an infinite plane wave in the fluid, incident at angle  $\theta$ , with frequency  $f$ .
- Solve the wave equation in each of the bulk materials, for plane waves of frequency  $f$ . This gives longitudinal waves in the fluid half-spaces above and below the plate, and waves of both longitudinal and transverse polarization within the plate.
- Satisfy the boundary conditions at the fluid-solid interfaces as follows.
- The requirement of continuity at all times and positions on the interfaces leads to Snell's law, i.e. all waves that are present at an interface must have the same value for the wavevector component in the plane of the interface (all waves must have the same value of  $k_x$ ). This implies that the wave fields can be generally expressed as a sum of partial waves, each of whose propagation angle is determined from the incident angle  $\theta$  by Snell's law.
- Ensure continuity of normal displacement and stress across each interface, which leads to equations that determine the amplitudes and relative phases of each of the partial waves in each material layer, and which in turn define the wave field in the plate and the reflected and transmitted waves. Solution of the boundary condition equations results in expressions for the reflection coefficient  $R$  and transmission coefficient  $T$  of the form (see, for example, [3-6]):

$$R = \frac{X_s X_t - \tau^2}{(X_s + i\tau)(X_s - i\tau)} \quad (1)$$

$$T = \frac{i\tau(X_s + X_t)}{(X_s + i\tau)(X_s - i\tau)}$$

where  $X_s$  and  $X_t$  are functions whose zeros are the eigenvalues that define the symmetric and antisymmetric (with respect to the mid-plane of the plate) vibrational modes of the free plate, known as Lamb modes. Thus, the equations  $X_s = 0$ ,  $X_t = 0$  define the Lamb wave dispersion curves of the free plate.  $\tau$  contains the effect of the fluid loading; it shifts the poles of the reflection (or transmission) coefficient off the real axis, thereby ensuring that the modes are leaky. A number of authors, including those to whom reference was made above, have studied the leaky guided waves in terms of the poles and zeros of the reflection coefficient. Equations (1) show how the reflection and transmission coefficients are related to the dispersion curves of the free plate.

- The finite extent of the incident beam can be taken into account by expressing it as an angular spectrum of plane waves (e.g. [7]) and the reflected and transmitted beams determined by summing over the effects of all the plane waves in the angular spectrum. If it is assumed that the transducer behaves as a simple circular piston, the angular spectrum is simply the Fourier transform of the circular aperture function. The angular spectrum method for representing the diffraction effects resulting from a finite aperture is particularly convenient here because it makes use of the plane wave solutions of the problem obtained as above.

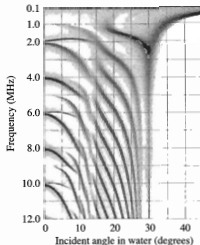


Figure 2. Calculated amplitude  $R(\theta, f)$  of the wave directly reflected from the surface of a 1.60 mm thick aluminium plate immersed in water, as a function of the incident angle  $\theta$  and frequency  $f$ . Black represents zero reflected signal, and white corresponds to total reflection. The transducers were 12mm diameter circular apertures.

The image in Figure 2 shows the amplitude of the reflection coefficient  $R(\theta, f)$  for a 1.60mm thick aluminium plate immersed in water. These are calculated results, assuming 12mm diameter circular transducers that behave as ideal pistons, and taking the transducer separation to be zero (i.e. direct reflection geometry).

Experimental data, in the form of sets of measurements of  $R(\theta)$  at various values of  $f$ , have been made and can be very well reproduced by these calculations. Data can be fitted by least-squares methods to determine the elastic and viscoelastic constants of the material, and their frequency dependence. An example of this will be given in the next section.

The results of Figure 2 illustrate some of the interesting physics of wave propagation in plates. The dark bands, where the reflected amplitude is small, are regions in which guided waves exist: most of the incident energy propagates down the plate and is re-radiated at larger values of  $x$ . These bands represent the dispersion curves of the guided waves, since the wavenumber of the guided waves is proportional to  $\sin \theta$ . If a similar calculation is done for  $x > 0$ , or of the transmission coefficient, the result is almost the inverse of Figure 2, since the guided waves now radiate energy rather than absorbing it. It can be seen from equations (1) that if the fluid loading is light ( $\tau$  small) the dark bands almost coincide with the dispersion curves of the free plate: the modes are then known as leaky Lamb modes.

Images of the form of Figure 2 contain more information than just the location of the dispersion curves, however. The shades of grey indicate how well a mode is coupled to the incident wave in the water at that point in  $(\theta, f)$  space, or how well it can be excited and detected. This is important if the modes are to be used for detecting defects in the plate. Some points of interest are listed below (see also, e.g., Auld [8], Pollard [9], Viktorov [10], or other texts on elastic waves in solids).

- The critical incident angle for longitudinal waves in aluminium, which is the incident angle for which the longitudinal wave is refracted parallel to the surface, is  $\sim 13.4^\circ$ . For transverse waves it is  $\sim 28^\circ$ . For  $\theta < 13.4^\circ$  the structure of the dispersion curves is quite complicated due to the coexistence within the plate of both longitudinal and transverse partial waves. For  $13.4^\circ < \theta < 28^\circ$  the dispersion curves have a simpler structure due to the presence of only the transverse waves - the longitudinal partial waves are now evanescent.
- There are light vertical bands in the regions corresponding to the longitudinal and transverse critical angles at all except low frequencies. This is a result of the total reflection of plane waves that occurs at these critical angles. The effect is less clear at low frequencies because of diffraction effects. The fixed aperture transducers generate more divergent beams at low frequencies, so, when the transducer is directed at the critical angle, only a relatively small proportion of the beam energy is incident at this angle.

- All of the modes except two converge to the transverse critical angle ( $\theta \sim 28^\circ$ ) at sufficiently high frequencies. Thus the high frequency limit of the phase velocity of all of these leaky Lamb modes is the bulk transverse wave velocity.
- The two modes at low frequency that do not converge at the transverse critical angle at high frequencies are the zeroth-order symmetric and antisymmetric Lamb modes, often referred to as  $S_0$  and  $A_0$ , respectively. The phase velocity of the antisymmetric mode  $A_0$  tends to zero at zero frequency, so the angle at which it is excited becomes large at low frequencies. This mode is the simple bending mode of the plate. The symmetric mode  $S_0$ , on the other hand, tends to a finite phase velocity, close to the bulk longitudinal wave velocity, at low frequencies: it resembles a longitudinal wave propagating down the plate.
- The two zeroth-order Lamb modes coalesce at about 2.5MHz to form Rayleigh waves, which are confined to the surfaces of the plate. The Rayleigh waves, which are dispersionless, are excited at  $\theta \sim 30^\circ$  and penetrate into the plate to a depth of the order of the wavelength. The zeroth-order Lamb modes may be thought of as the symmetric and antisymmetric couplings of a Rayleigh wave propagating on each surface of the plate. At high frequency they are effectively independent of each other, but as the frequency is decreased they penetrate further into the plate and their coupling increases, producing a splitting at  $f \sim 2.5$ MHz.
- At high frequencies, only the Rayleigh wave on the incident surface is excited. For infinite plane wave excitation, this wave will absorb no net energy from the incident beam: all of the energy that goes into the Rayleigh wave will be re-radiated and will appear as reflected energy, albeit with a phase shift to account for the re-radiation delay. For the finite beam case shown in Figure 2, the fixed aperture transducer approaches a plane wave source at high frequencies, so the amount of energy removed from the beam by the Rayleigh wave decreases as the frequency is increased.

To show how information such as that in Figure 2 can be used, attention is now turned to the case of a multi-layered plate—an adhesive bond.

### 3. LEAKY GUIDED WAVES IN AN ADHESIVELY-BONDED ALUMINIUM PLATE

Consider now a structure that consists of two aluminium sheets bonded together by a thin epoxy adhesive layer. The waves propagating in such a three-layered structure can be calculated using the same general procedure outlined in the previous section, but in this case there are four partial waves in each solid layer. The wavenumbers and propagation directions of these partial waves are determined by the elastic constants of the layer material and Snell's law—the  $x$ -components of the wavenumbers of all partial waves in all layers are equal. The (complex) amplitudes of the partial waves are determined by the boundary conditions, bearing in mind that in this case there are additional boundary conditions

that must be satisfied at the two solid-solid interfaces within the plate. For a well-bonded interface there are four such conditions: continuity of normal and tangential particle displacement (or velocity) and of normal and shear stress across the interface.

Figure 3 shows the amplitude of the reflection coefficient  $R(\theta, f)$  for a water-immersed bonded plate typical of structures encountered in airframes. These results are directly comparable with those for the aluminium sheet shown in Figure 2. Figure 4 shows the results of experimental measurements of the reflected amplitude from a bonded plate similar to that for which the calculations of Figure 3 were performed. These results give confidence that the computational model is a reasonable one.

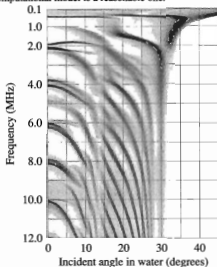


Figure 3. Calculated amplitude  $R(\theta, f)$  of the wave directly reflected from the surface of an adhesively-bonded aluminium plate immersed in water, as a function of the incident angle  $\theta$  and frequency  $f$ . Black represents zero reflected signal, and white corresponds to total reflection. The plate consists of two sheets of 1.60mm thick aluminium, well-bonded by a 0.25mm thick layer of epoxy adhesive. The transducers were 12mm diameter circular apertures.

It is apparent that, over much of the  $(\theta, f)$  space shown in Figures 2 and 3, the general pattern of the dispersion curves is very similar for the single aluminium sheet and the bonded plate. The reason for this is that in much of the region the bonded plate behaves like two identical resonators (the Al sheets) coupled by a relatively soft spring (the adhesive layer). There are, however, regions where the structure of the dispersion curves for the two cases differ significantly. These regions are of great interest, because it is expected that here the modes will be most sensitive to the properties of the bonding layer.

In particular, attention is drawn to the following regions of difference.

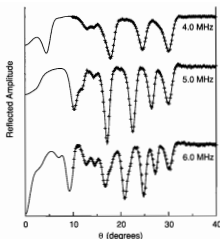


Figure 4. Measured amplitude of waves directly reflected from the surface of an adhesively-bonded aluminium plate immersed in water, as a function of the incident angle  $\theta$ , at the frequencies indicated. The crosses are the results of measurements made using long ( $\sim 100 \mu\text{s}$ ) tone-burst pulses to approximate continuous waves. The solid lines are the results of a least squares fit, to all three sets of data simultaneously, using the model described in the text. The plate consisted of two sheets of 1.60mm thick 2024 aluminium, well-bonded by a 0.24mm thick layer of epoxy adhesive (FM-73, American Cyanamid). Two 12mm diameter, 5MHz centre frequency transducers were used.

- The existence of a mode in the bonded plate at  $\sim 0.5\text{MHz}$ , over a wide range of  $\theta$ , for which no equivalent exists for the single aluminium sheet. At normal incidence this is a (symmetric) thickness resonance of the bonded plate, with most of the strain in the adhesive layer because of its relative softness. It is a symmetric mode that is derived from the zero-order antisymmetric Lamb mode of the single sheet: the motion in each of the Al sheets is antisymmetric while that in the adhesive layer is symmetric. Because the motion in the adhesive layer is symmetric, the stress in this layer is mainly normal to the plate surface. The shear stress introduced at higher incident angles is confined mainly to the Al sheets.
- Sharp, narrow modes occur in the single aluminium sheet at and near normal incidence ( $\theta = 0$ ) at 2, 6, 10, ... MHz, which are not present in the bonded plate. These are thickness-shear resonances in the aluminium, and they are strongly damped by the presence of a bonded adhesive layer on the aluminium surface. These modes and their excitation have been described in more detail previously [11], and they will be encountered again below. They are generated by mode conversion of components of the incident beam that are not exactly normal to the surface, and they are "pumped" by the adjacent symmetric longitudinal resonance in each case.

- A broad, weak minimum that occurs for the bonded plate at small incident angles near  $f = 4.8$  MHz. This is the thickness resonance of the adhesive layer.
- A number of transverse modes of the bonded plate, particularly in the region around  $\theta \sim 20^\circ$ ,  $f \sim 3$  MHz, are associated with the adhesive layer.

#### 4. DETECTION OF DEFECTS IN A BONDED PLATE

The use of leaky guided waves for detecting defects in planar bonded structures requires a means of determining which modes are sensitive to particular defects. This can be done qualitatively by consideration of the stress and strain distributions generated by a particular mode, and the way in which the ideal and defective materials would respond to these distributions [12,13]. The computational model described above can be used to calculate stress and strain distributions associated with particular modes for use in such analyses. To take a simple example, a closed disbond, coplanar with the plate surface, would not be detectable in a compressive normal stress, though it might be if the stress was tensile and sufficiently large. However, a shear stress applied across such a defect would be expected to produce a significantly different response from that in the absence of the disbond.

Images of 2D data sets such as those shown in Figures 2 and 3 suggest a simple empirical method for the identification of modes that are sensitive to planar defects. The defect is assumed to be infinite in lateral extent. It is included in the numerical model and an image of the reflection or transmission coefficient of the defective structure obtained. The difference between this image and a comparable one for the ideal structure can then be found by subtraction of the images, and regions of the  $(\theta, f)$  parameter space where there are significant differences can be immediately identified. Even if the real defect is not large, the modes that are perturbed by the infinite model of the defect will be scattered by one of finite extent. Two examples of this procedure and its results will be very briefly described.

##### 4.1 Detection of a closed disbond

The first example is that of a closed disbond, a situation that occurs when there is delamination of the adhesive from the metal, perhaps as a result of poor surface preparation, surface contamination or in-service water ingress and interfacial corrosion. The bond is held tightly closed, perhaps by structural stresses, but it has no shear strength. This is a defect that cannot normally be detected by traditional through-transmission or pulse-echo ultrasonic inspection techniques. It is incorporated into the computational model by relaxing the condition that the tangential displacement and shear stress be continuous across the metal/adhesive interface.

The results are shown in Figure 5, which corresponds to the case of a disbond at the upper (referred to the orientation shown in Figure 1) aluminium/adhesive interface. Similar results are found for a disbond at the lower interface. The difference image shows that the most significant differences are near normal incidence at  $f \sim 2, 6, 10$  MHz (in fact, the

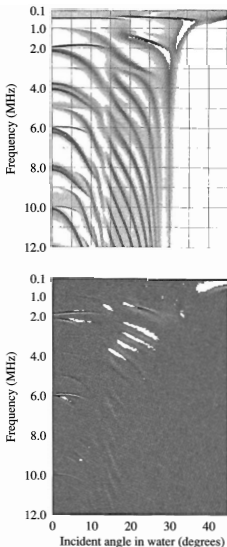


Figure 5. Calculated amplitude  $R(\theta, f)$  of the wave directly reflected from the surface of an immersed, adhesively-bonded aluminium plate with a closed disbond at the upper aluminium/adhesive interface, as a function of incident angle  $\theta$  and frequency  $f$ . The upper image is comparable to Figure 3 while the lower one is the difference between the images for the disbonded plate (upper) and the well-bonded plate (Figure 3).

resolution of the images of Figure 5 is not sufficient to show the strong but very narrow modes that occur at and close to normal incidence at 6 and 10 MHz). Further investigation shows that, in the presence of the disbond, the symmetric thickness-shear resonances of the single aluminium plate, referred to above, have reappeared in the disbonded sheet.

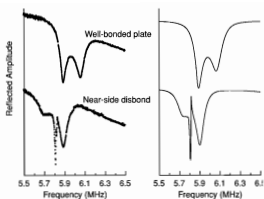


Figure 6. Reflected spectra for two different plates, as described in the text, for normal incidence ( $\theta = 0$ ). Spectra measured using a 12mm diameter, 5MHz centre frequency transducer are on the left, with calculated spectra on the right. The sloping baselines of the measured spectra are due to the frequency response of the transducer, which is not included in the calculations.

This is also true if the lower sheet is disbanded.

These results have been verified experimentally, a typical example being shown in Figure 6. In this case the closed disbond was simulated by fabricating a bonded plate with a release agent in one of the aluminium/epoxy interfaces, so that it was readily delaminated after curing. In order to exclude air from the disbond, the two parts of this plate were clamped together under water, trapping a thin water film in the delaminated interface. The sharp feature at approximately 5.8MHz in Figure 6 is a result of the aluminium thickness-shear resonance referred to above. Although it is difficult to see in this figure, the measured data in this region show that this mode is broadened by the small rolling-induced anisotropy of the aluminium sheet. A practical technique based on the detection of these modes has been developed [11].

#### 4.2 Detection of reduced elastic modulus of the adhesive

The second example is of detection of a degraded material property rather than of a discrete defect. Reduced elastic moduli of the adhesive may result from, for example, inadequate curing of the adhesive, incorrect adhesive composition, microcracking within the adhesive, etc. This condition is incorporated into the model by simply reducing the values of the elastic constants of the adhesive layer, and the results are given in the form of the difference image in Figure 7.

It can be seen that most of the modes near normal incidence show sensitivity to this condition, since they are essentially thickness resonances of the plate. However, this is not very useful in practice since there is considerable ambiguity with bond thickness: the observed sensitivity is almost completely removed if the adhesive layer thickness is reduced in the same proportion as the elastic constants. Since, in practice, the exact thickness of the bond is generally not

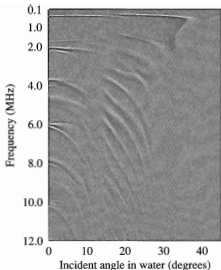


Figure 7. Calculated amplitude  $R(\theta, f)$  of the wave directly reflected from the surface of an immersed, adhesively-bonded aluminium plate with the elastic moduli of the adhesive reduced by 10% from the values used to calculate the data in Figure 3, as a function of the incident angle  $\theta$  and frequency  $f$ . The image shown is of the difference between the data for the reduced modulus plate and that for the well-bonded plate (Figure 3).

known, the thickness resonances cannot be used to measure the adhesive properties.

There is less ambiguity and substantial sensitivity, however, in the 0.5MHz symmetric mode derived from the  $A_1$  modes of the aluminium sheets, described in Section 3. The frequency of this mode depends on the adhesive layer thickness, but not in the same ratio, so this mode, possibly in combination with measurements of thickness resonances, may be used to measure adhesive modulus.

## 5. CONCLUSIONS

A brief introduction has been given to some features of the propagation of leaky guided waves in multi-layered planar structures immersed in a fluid, and the utility of these waves for characterisation of structures such as adhesively bonded joints has been illustrated. While the emphasis in this paper has been on computational results, a parallel experimental program has been carried out and the results presented here have all been verified by measurement. The approach has been to use the generality and flexibility of water immersion techniques to determine how a particular defect, or class of defects, may be detected, and to use this information to design a specific practical inspection technique.

The calculations outlined here are part analytical and part numerical. Solutions of the wave equations for the various materials, and Snell's law of spatial continuity, are used to determine the nature and orientation of the partial waves that are used as basis functions for numerical solution of the

boundary condition equations. This approach has the advantage over a fully numerical method, such as a finite element calculation, of providing greater insight into the physics of the wave propagation. The advantage over a fully analytical solution, which is possible for the single layer plate (see equations (1)) is that it can be readily extended to the case of multi-layered plates.

This method can also be extended to describe wave propagation in multi-layered anisotropic materials, such as carbon fibre composite laminates [2]. Work on these materials has been done within this laboratory, to find methods to detect inclusions of foreign materials embedded in composite laminates [14,15]. Material anisotropy adds considerable complexity to both the model and the results, but the general principles are the same as those presented here for isotropic materials.

Current theoretical and experimental work in this program is aimed at extending the approach outlined here to describe the non-linear propagation of large amplitude leaky guided waves, in the limit of weak non-linearity. It is known that some classes of material conditions, such as fatigue microcracking, and some microstructural properties such as hardness, have a much greater effect on the non-linear response of materials than on linear wave propagation. There are also indications, not yet unambiguously confirmed, that some mechanisms that lead to weak adhesion of bonded joints and surface coatings may lead to enhanced material non-linearity. The program of non-linear guided wave propagation in layered structures is aimed at investigating these problems. The non-destructive detection of weak adhesion is currently not possible.

## REFERENCES

- [1] S.J. Bowles and C.M. Scala, "Ultrasonic Lamb waves for NDT of materials" Non-Destructive Testing - Australia **33**, 164-8 (1996).
- [2] D.E. Chimenti, "Guided waves in plates and their use in materials characterization" Appl. Mech. Rev. **50**, 247-84 (1997).
- [3] A. Schoch, "Schall Durchgang durch Platten" [Sound transmission through plates] *Acustica* **2**, 1-18 (1952).
- [4] L.E. Pitts, T.J. Plona and W.G. Mayer, "Theoretical similarities of Rayleigh and Lamb modes of vibration" J. Acoust. Soc. Am. **60**, 374-7 (1976).
- [5] R. Fiorito, W. Madigosky and H. Oberall, "Resonance theory of acoustic waves interacting with an elastic plate" J. Acoust. Soc. Am. **66**, 1857-66 (1979).
- [6] O. Lenoir, J. Duclos, J.M. Conoir and J.L. Izbecki, "Study of Lamb waves based upon the frequency and angular derivatives of the phase of the reflection coefficient" J. Acoust. Soc. Am. **94**, 330-43 (1993).
- [7] J.W. Goodman, *Introduction to Fourier Optics* McGraw-Hill, New York (1968).
- [8] B.A. Auld, *Acoustic Fields and Waves in Solids* Krieger, Florida (1990). (2 volumes)

- [9] H.F. Pollard, *Sound Waves in Solids* Pion, London (1977).
- [10] I.A. Viktorov, *Rayleigh and Lamb Waves* Plenum, New York (1967).
- [11] D.C. Price and B.J. Martin, "Ultrasonic inspection of bonded metal plates using pulse-echo spectroscopy" Non-Destructive Testing - Australia **30**, 139-42 (1993).
- [12] J.J. Ditre, J.L. Rose and G. Chen, "Mode selection criteria for defect detection optimization using Lamb waves" Review of Progress in Quantitative Nondestructive Evaluation **11**, 2109-15 (1992).
- [13] A. Pilarski and J.L. Rose, "Lamb wave mode selection concepts for interfacial weakness analysis" J. Nondestruct. Eval. **11**, 237-49 (1992).
- [14] J.A. Ogilvy, "A model for the inspection of composite plates" *Ultrasonics* **33**, 85-93 (1995).
- [15] J.A. Ogilvy, D.C. Price and B.J. Martin, "Horizontally polarised shear wave resonances in carbon-fiber/epoxy composites" Review of Progress in Quantitative Nondestructive Evaluation **14**, 1249-56 (1995).



NOISE CONTROL  
AUSTRALIA PTY. LTD.

ADJ 078 415 639

**Committed to Excellence in  
Design, Manufacture & Installation of  
Acoustic Enclosures, Acoustic Doors,  
Acoustic Louvres & Attenuators**

### SUPPLIERS OF EQUIPMENT FOR:

PROJECT: Conservatorium of Music  
CLIENT: Austaff Air Conditioning

**70 TENNYSON ROAD  
MORTLAKE NSW 2137**

**Tel: 9743 2413**

**Fax: 9743 2959**

*A Sustaining Member of the Australian Acoustical Society*